TiN_xO_y coatings facilitate the initial adhesion of osteoblasts to create a suitable environment for their proliferation and the recruitment of endothelial cells

Biomedical Materials

PAPER

TiN_xO_y coatings facilitate the initial adhesion of osteoblasts to create a suitable environment for their proliferation and the recruitment of endothelial cells

RECEIVED
13 September 2016

REVISED
9 December 2016

ACCEPTED FOR PUBLICATION
9 January 2017

PUBLISHED
28 February 2017

M Moussa[1], O Banakh[2], B Wehrle-Haller[3], P Fontana[4], S Scherrer[1], M Cattani[1], A Wiskott[1] and S Durual[1]

[1] Division of fixed prosthodontics and biomaterials, University clinics of dental medicine, University of Geneva, Switzerland
[2] Institute of Applied Microtechnologies, Haute Ecole Arc Ingénierie (HES-SO), Eplatures-Grise 17, CH-2300 La Chaux-de-Fonds, Switzerland
[3] Department of cell physiology and metabolism, University medical center, University of Geneva, Switzerland
[4] Division of angiology and haemostasis, University of Geneva, HUG and Geneva Platelet group, Switzerland

E-mail: stephane.durual@unige.ch

Keywords: titanium-nitride-oxide coating, osteoblast, focal adhesion, osseointegration, angiogenesis

Abstract

Titanium-nitride-oxide coatings (TiN_xO_y) improve osseointegration of endosseous implants. The exact mechanisms by which these effects are mediated are poorly understood except for an increase of osteoblast proliferation while a high degree of differentiation is maintained. One hypothesis holds that TiN_xO_y facilitates the initial spreading and adhesion of the osteoblasts. The aim of this work was to investigate the molecular mechanisms of osteoblast adhesion on TiN_xO_y as compared to microrough titanium SLA. A global view of the osseointegrative process, that is, taking into account other cell groups, especially endothelial cells, is also presented. To this aim, gene expression and focal adhesion analysis, cocultures and wound assays were performed early after seeding, from 6 h to 3 days. We demonstrated that TiN_xO_y coatings enhance osteoblast adhesion and spreading when compared to the standard microrough titanium. The integrin $\beta 1$, either in association with $\alpha 1$ or with $\alpha 2$ plays a central role in these mechanisms. TiN_xO_y coatings optimize the process of osseointegration by acting at several levels, especially by upregulating osteoblast adhesion and proliferation, but also by supporting neovascularization and the development of a suitable inflammatory environment.

Introduction

Among the wide range of options that were proposed in the last decade to optimize the osseointegration of titanium implants, subtractive processes, that is, those imparting a 'moderate' micro-roughness to the surface, were among the most successful [1–3]. Sand-blasting followed by acid etching (in their various declinations) produces a multiscale surface roughness —ranging from craters of 15–20 μm to micro-pits 1–3 μm in depth—which is most suitable to mesenchymal stem cell and osteoblast proliferation and differentiation [3]. Refinements such as HA blasting and conditioning in N_2 protective atmosphere further improved the performance of the implant surface during osseointegration [4].

In the context of surface optimization, titanium oxynitride thin films (TiN_xO_y) deposited by plasma vapor deposition appear as beneficial to bone healing. First, the high resistance of these coatings allows their application in a thin layer (100–200 nm) which will not affect the substrate's microroughness [5]. Second, in comparison with the bare standard SLA surface (sand blasting and acid etching), TiN_xO_y coatings accelerate osseointegration by about 50% during the first month of healing both *in vitro* and *in vivo* [5, 6]. Third, this effect is independent of the substrate on which the films are deposited [6, 7] and gradually increase with the O content until an optimum is reached between the coatings' mechanical- and biological properties [8]. Fourth, TiN_xO_y do not alter the high thrombogenic potential of SLA substrates.

It appears that the TiN_xO_y coating affects the early stages of cell adhesion by acting as a catalyst for cell attachment and spreading [8]. During the process of osseointegration, the cells do not adhere on the

titanium surface directly but on an adsorbed layer of macromolecules (mainly collagens and fibronectin (FN)) which establish a preliminary extracellular matrix (ECM). At later stages, this ECM is remodeled by the cells after adhesion has taken place [9]. Cell adhesion to ECM ligands is primarily mediated by integrins (ITG). Following ligand binding, integrins cluster and associate with cytoskeletal elements to form focal adhesions, that is, supramolecular assemblies of structural and signaling proteins that provide anchorage and activate signaling cascades regulating cell cycle progression and differentiation [10]. In this context, osteoblasts mostly express the integrin subunits $\alpha1$, $\alpha2$, $\alpha3$, $\alpha4$, $\alpha5$, $\alpha6$, αv, $\beta1$, $\beta3$ and $\beta5$ [11]. ITG $\alpha2\beta1$ and to a lesser extent $\alpha1\beta1$ are clearly associated with osteoblast maturation and differentiation on microrough surfaces, as shown by silencing (siRNA) of $\alpha1$, $\alpha2$ and $\beta1$ mRNA [12, 13]; ITG $\alpha1\beta1$ may also be implied in the proliferation mechanisms [14, 15]. In contrast, the initial mechanisms of osteoblast adhesion on titanium, i.e. during the first 24 h after seeding, are not clear, although ITG $\alpha5\beta1$ was mentioned as a key element but only from day 3 [16].

Besides osteoblast adhesion to the implant's surface, osseointegration also depends on neovascularization for the supply of nutrients and growth factors. Tight communication processes were demonstrated between endothelial cells and osteoblasts during osteogenesis. For instance, endothelial cells can stimulate the proliferation and differentiation of osteoblasts via the secretion of BMP2, endothelin-1 or insulin growth factor [17–19]. Conversely, osteoblasts are capable of synthetizing VEGF, a known activator of endothelial cell proliferation and differentiation [20–22].

In light of the potential of TiN_xO_y coatings in terms of osseointegration and with the hypothesis that TiN_xO_y facilitates the initial stages of osteoblast adherence and spreading, the aim of the present work was twofold. First, to further investigate the mechanisms of cell adhesion with a focus on the main osteoblastic integrins and, second, to assess the relations between osteoblasts and other cells involved in the bone regeneration process, more specifically endothelial cells.

Materials and methods

Substrates

Test plates (11 mm × 11 mm × 0.635 mm) made of Ti Cp-IV (Signer Titanium, Switzerland) were SLA textured using previously described procedures (resulting R_a: 2.49 ± 0.34) [5]. The plates were coated with a 3000 Å ± 10% layer of TiN_xO_y by reactive direct current magnetron sputtering. The sputtering process and coating characterization were described elsewhere [23]. The film deposition on SLA surfaces did not modify the microroughness parameters [5]. The film composition was set as follows: Ti 28% at; N 16% at; O 56% at; N/Ti 0.56; O/Ti 1.96. This stoichiometry balances the mechanical (material resistance) versus the biological (enhancement of osteointegration) properties [8]. For the sake of simplicity, bare substrates and coated substrates will be referred as Ti-SLA and TiN_xO_y hereafter.

Cells

HOS (CRL-1543^{TM}) and EA.hy926 (CRL-2922^{TM}) cells were obtained from ATCC and maintained in MEM medium (Life Technologies, USA) supplemented with 10% fetal calf serum (Eurobio, France), 1% penicillin/streptomycin/fungizone (Life Technologies), 2% HEPES (Life Technologies). Primary osteoblasts (hOBs) were isolated from alveolar bone taken from healthy patients undergoing routine dental extraction [5] and further cultured in DMEM medium (Life Technologies) using the same supplementation as described above. For all experiments, the cells were cultured in 24-well plates in which the Ti-SLA and TiN_xO_y plates were immersed.

Cell culture

Proliferation assay. HOS cells were cultured on SLA-textured-Ti (Ti-SLA) and SLA-textured-TiN_xO_y-coated-Ti (TiN_xO_y) at a density of 2600 cells cm^{-2}. Cells were cultured for 21 days in triplicate ($n = 18$). Within each run, Resazurin assays and RNA extractions were performed at days 2–3, 7, 14 and 21.

The same procedure was repeated for the EA.hy926 cells, except for RNA extractions.

Resazurin assay

Resazurin (Sigma-Aldrich, USA) was added to the culture media to a concentration of 0.01 mg ml^{-1} after which the cells were maintained at 37 °C/5% CO_2 for 4 h. The supernatants were removed and their absorbance was measured at 570 nm on an ELISA plate reader (background OD 630 nm).

Coculture and flow cytometry. HOS and EA.hy926 cells were seeded on Ti-SLA or TiN_xO_y plates according to a ratio HOS/EA: 1/5 (2600 and 13 000 cells cm^{-2}. At day 1, 3, 6 and 8, the cells were detached by trypsinisation and stained with PE-CD31 antibody (Mouse Anti-Human, CL L133.1, BD Biosciences). Cells were then analyzed on a BD-C6 flow cytometer (BD Accuri,USA) and the relative proportions of EA and HOS were calculated according to the postulate that EA cells express CD31 whereas HOS cells do not. The experiment was repeated three times in triplicate ($n = 9$).

Migration assay. HOS and EA.hy926 cells were seeded on 6 well polystyrene plates until they reached confluence. A wound was then created (scratching with a pipette tip) as a stripe bisecting the cell layer. Conditioned media obtained from HOS cells grown on Ti-SLA or TiN_xO_y for 1 day (stored at −20 °C from previous experiments) were then applied on wounded

cells for 2 days (medium changed daily) and the wound recovery was evaluated under an inverted microscope (Axiovert 100 M) coupled to a camera (Orca 9742–95; Hamamatsu Photonics). The experiment was repeated three times in triplicate.

RNA isolation and RT-PCR analysis

The total cellular RNA was extracted with commercial extraction kits (Peqgold Trifast, Peqlab, Germany) according to the manufacturer's instructions. First-strand cDNAs were synthesized using superscript-II reverse transcriptase (Life Technologies) and were then amplified by PCR using the following primers (5′−3′) (Microsynth, CH): hRUNX2 (238 bp): forward, ccggaatgcctctgctgttatga, reverse, actgaggcggtcagagaacaaact; h alkaline phosphatase (278 bp, ALP): forward, tgcagtacgagctgaacaggaaca, reverse, tccaccaaatgtgaagacgtggga; h osteoprotegerin (409 bp, OPG): forward, ggggaccacaatgaacaagttg, reverse, agcttgcaccactccaaatcc; collagen 1A1(348 bp): forward: ccctccccagccacaaagagtct, reverse: gggtgactctgagccgtcgg; Integrin B1(322 bp): forward: atgaatgaaatgaggaggattacttcg, reverse: aaaacaccagcagccgtgtaac; integrin B3 (281 bp): forward: aggatgactgtgtcgtcagat, reverse: ggtagacgtggcctctttataca; Integrin A1 (210 bp): forward: gtgcttattggttctccgttagt, reverse: gcccacaagccagaaatcct; integrin A2 (166 bp): forward: gcaactggttactggttggtt, reverse: gaggctcatgttggttttcatct; integrin Av (305 bp): forward: actgggagcacaaggagaacc, reverse: ccgcttagtgatgagatggtc; Integrin A5 (163 bp): forward: gcctgtggagtacaagtcctt, reverse: aattcgggtgaagttatctgtgg; fibronectin (295 bp): forward: gctaagcagttggtggtgca, reverse: gaactatgatgccgaccagaa PCR was performed in an automated thermal cycler (Lifepro, Bioer, CN) (denaturation: 94 °C, 30 s; annealing: 55 °C, 30 s; extension: 72 °C, 30 s).

qPCR analyses for IL6, 8, 11 and 10 were run on a real time PCR machine (Steponeplus, Life Technologies-Applied Biosystems) using taqman assays (Life Technologies), according to the manufacturer's instructions.

Immunostainings and confocal microscopy

Fluorescent immunostaining. hOBs and HOS cells were plated for 6 and 24 h on Ti-SLA and TiN_xO_y plates before fixation with PBS/PFA4% followed by washing (PBS), permeabilization and blocking with PBS/BSA1%/$TritonX_{100}$ 0.2% for 30 min. The primary antibodies were then incubated for 30 min in PBS/BSA2% and after three washings with PBS, an additional 30 min incubation with secondary antibodies was performed. Finally the samples were processed for confocal laser scanning microscopic analysis (Zeiss Axio Imager M2, HXP120C fluorescence lamp for widefield eyepiece visualization at room temperature, Plan-Apochromat 63x/1.4 Oil immersion objective, Zen 2010b software—service pack1).

The adjustments of the scanning microscope were set on an initial experiment in which we considered three cell samples on Ti-SLA and three cell samples on TiN_xO_y with an optimal and unsaturated mean intensity of fluorescence. These adjustments were applied to all the following samples. The autofluorescence of the bare surfaces was also evaluated and was minor and equivalent. The following antibodies were used for the different experiments; the dilutions were the same for all the samples: mouse mAb anti–chicken paxillin (clone 349; BD; reacting with mouse paxillin, dil. 1/300), rat mAb anti–mouse β1 integrin (clone 9EG7; BD, dil. 1/3000), mouse mAb antivinculin (V9131; Sigma-Aldrich, dil. 1/1000), DyLight 549–conjugated goat anti–mouse (Jackson ImmunoResearch Laboratories, Inc., dil. 1/2000), rabbit polyclonal antibody anti-mouse/human/rat α1 integrin conjugated to Cy5 (ABIN677487, antibodies-online GmbH, dil. 1/300), mouse monoclonal (2B6) antibody anti-human α2 integrin (ABIN561540, antibodies-online GmbH, dil. 1/3000), Goat anti-mouse IgG (H + L) Cy5-AffiniPure (Jackson ImmunoResearch Laboratories, Inc., dil. 1/300), Fluorescein (FITC) AffiniPure Goat Anti-Rat IgG (H + L) (Jackson ImmunoResearch Laboratories, Inc., dil. 1/500).

Immunostaining quantification. Immunostaining was quantified with the Image J software (NIH, USA) using the ROI manager plugin. The structures of interest (SOI) were delimited manually for each single cell or group of cells and the fluorescence intensities for each channel were calculated per cell and expressed as mean +/− sem. Artifacts caused by the unspecific adsorption of antibodies onto the substrate were excluded from the computations as well as saturated areas. For ITG β1, a total of 18 plates harboring 2–20 cells/section was assessed resulting in the delimitation of 57 SOI for Ti-SLA 6 h, 60 SOI for Ti-SLA 24 h, 60 SOI for TiN_xO_y 6 h and 62 SOI for TiN_xO_y 24 h. For ITG α1, a total of 6 plates harboring 1–18 cells/section was assessed resulting in the delimitation of 15 SOI for Ti-SLA 6 h, 16 SOI for Ti-SLA 24 h, 16 SOI for TiN_xO_y 6 h and 17 SOI for TiN_xO_y 24 h. For ITG α2, a total of 6 plates harboring 1–15 cells/section was assessed resulting in the delimitation of 20 SOI for Ti-SLA 6 h, 20 SOI for Ti-SLA 24 h, 20 SOI for TiN_xO_y 6 h and 20 SOI for TiN_xO_y 24 h. For Paxillin, a total of 6 plates harboring 1–14 cells/section was assessed resulting in the delimitation of 27 SOI for Ti-SLA 6 h, 24 SOI for Ti-SLA 24 h, 36 SOI for TiN_xO_y 6 h and 31 SOI for TiN_xO_y 24 h. For Vinculin, a total of 6 plates harboring 1–16 cells/section was assessed resulting in the delimitation of 22 SOI for Ti-SLA 6 h, 41 SOI for Ti-SLA 24 h, 24 SOI for TiN_xO_y 6 h and 36 SOI for TiN_xO_y 24 h. The outcome data were pooled for each assay.

Colocalization analysis. Confocal images of anti β1 integrin FITC Goat Anti-Rat and antipaxillin, antivinculin, DyLight 549 fluorescence, anti-α1 integrin conjugated to Cy5, anti α2 integrin Cy5-AffiniPure

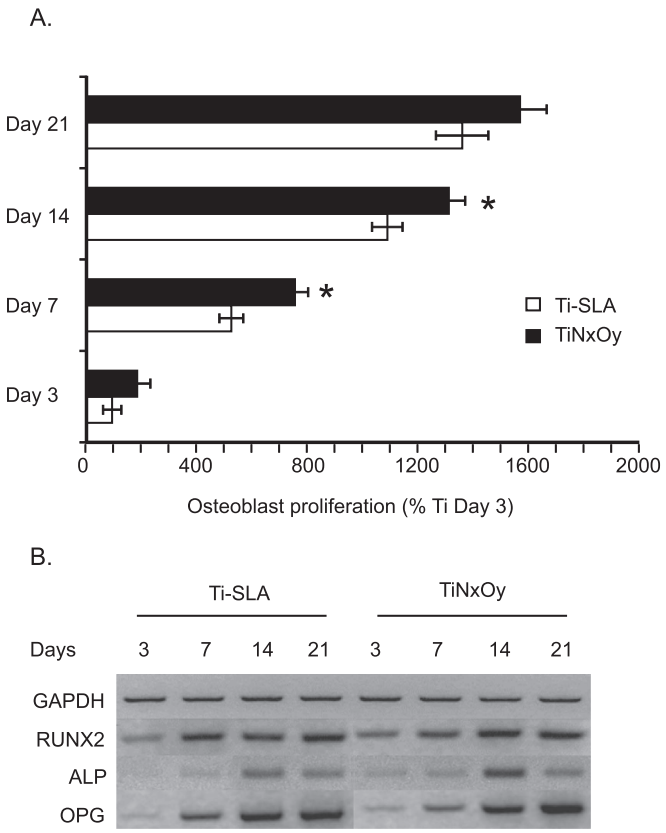

Figure 1. Proliferation and differentiation of HOS grown on Ti-SLA and TiN_xO_y from day 3 to 21. (A) Resazurin assay. Data (mean $\pm$ sem, $n = 12$) expressed as percent of control (i.e. day 3, Ti-SLA). White bars: Ti-SLA; black bars, TiN_xO_y. *: $p < 0.05$ as compared to Ti-SLA at the same day. (B) Semi quantitative RT-PCR analysis for runx2, ALP and OPG genes. (One experiment representative of six).

were acquired sequentially. The colocalization was determined from the total cells on the plates using the Imaris software (Bitplane, CH). Pearson's colocalization coefficients were calculated with fixed thresholds for each series of samples belonging to the same experiment. ($n = 6$ plates for $\alpha1\beta1$, $\alpha2\beta1$, $\beta1$-paxillin, $\beta1$-vinculin at 6 h and 24 h).

Statistical analysis

Differences in gene expression, fluorescence intensity, colocalization and proliferation between cells grown on Ti versus TiN_xO_y plates were assessed using Student's t test; significance levels were set to $p \leqslant 0.05$. The Gaussian distribution was previously verified using the Shapiro–Wilk W test. All the data sets were normal with probabilities in excess of 0.05.

Results

HOS proliferation and differentiation

The HOS osteoblastic cell line was used in the present assay series. As a first step, we verified whether HOS cells duplicated the results obtained on TiN_xO_y with primary osteoblasts in terms of proliferation and differentiation [5, 7]. To this effect, HOS cells were grown on Ti-SLA and on TiN_xO_y-coated plates. The proliferation was measured with resazurin from day 3 to 21. As shown in figure 1(A), on both surfaces, the cells proliferated and multiplied by ca. sixteen times at day 21. However, the proliferation on TiN_xO_y at days 7 and 14 was significantly increased (by 1.4- and 1.3-times, respectively) as compared to Ti-SLA.

We also assessed the differentiation of HOS cells by analyzing the expression of typical osteoblastic genes by RT-PCR, that is, alkaline phosphatase (ALP), RUNX2 and osteoprotegerin (OPG). The same profiles of expression were observed on Ti-SLA and TiN_xO_y coatings, without notable differences. RUNX2 and OPG gradually increased from day 3 to 21 whereas ALP increased up to day 14 before decreasing slightly (figure 1(B)).

Expression of HOS cells integrins

We analyzed the gene expression of ITG subunits in HOS cells grown on Ti-SLA and TiN_xO_y at days 1 and 3. As shown in figure 2, ITG$\beta1$ was substantially increased on TiN_xO_y at days 1 and 3 when compared to Ti-SLA, on which a decrease was observed. In contrast, ITG$\beta3$ increased slightly only at day 3. ITG$\alpha1$ and $\alpha2$ increased at day 1 and remained unchanged at day 3, contrary to ITGαv and $\alpha5$ which were stable at day 1 and increased slightly at day 3. The genes for FN and collagen 1α (COL1α) (i.e. the main components of the ECM) were also analyzed. COL1α

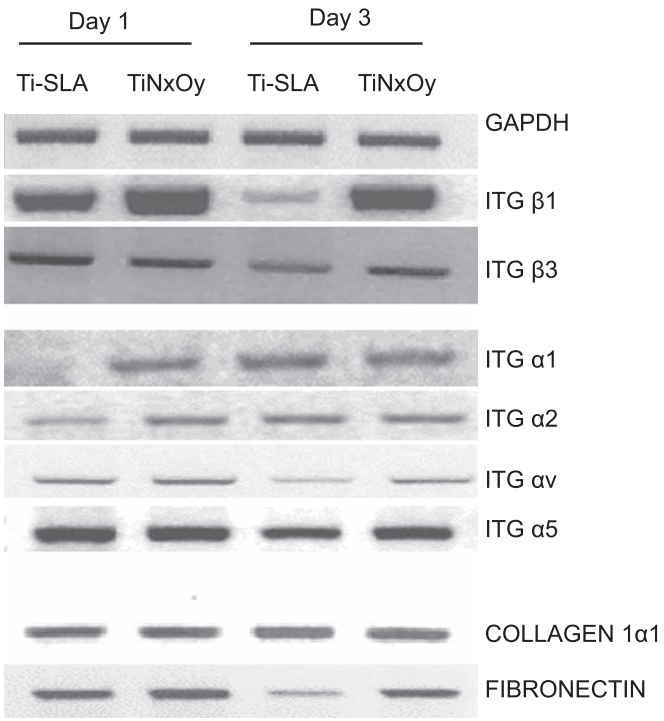

Figure 2. Gene expression of integrins (ITG) (β1, β3, α1, α2, αv, α5), collagen 1α1 and fibronectin in HOS seeded on Ti-SLA and TiN_xO_y at day 1 and 3 (1 experiment representative of 4).

expression was equal on both surfaces at day 1 and 3, whereas FN expression, which was the same at day 1 on both surfaces, thereafter decreased on Ti-SLA but remained stable on TiN_xO_y.

Adhesion mechanisms

To elucidate the early mechanisms of cell adhesion on TiN_xO_y as compared to Ti-SLA, we performed immunostainings at 6 and 24 h, focusing on those ITG subunits for which the expression differed at day 1. The cells were first co-stained using primary antibodies in four combinations (α1/β1, α2/β1, Vinculin/β1 and Paxillin/β1) before adding secondary antibodies tagged with fluorophores: FITC (green: ITG β1), Cy-5 or Dylight549 (red: ITG α1, α2, Vinculin and Paxillin). Fluorescent intensities (i.e. reflecting target–protein quantities), colocalizations (i.e. reflecting target–protein interactions) and focal adhesions were quantified. The gene expression analysis was confirmed as ITGβ1 fluorescence was increased by ca. 1.5 times on TiN_xO_y at 6 and 24 h (figures 3–6 E) when compared to Ti-SLA while the response of ITGα1 and α2 was essentially the same (figures 3 E and 4 E). ITGβ1 (figures 3–6, A2, B2, C2 and D2), ITGα1 (figure 3 A3, B3, C3 and D3) and ITGα2 (figure 4 A3, B3, C3 and D3) were uniformly distributed on the cells' surfaces, either at 6 h or 24 h. The cells spread and elongated more on TiN_xO_y than on Ti-SLA as early as 6 h after seeding (figures 3–6, A2, B2, C2 and D2). ITGβ1 was colocalized with ITGα1 and ITGα2 on both surfaces. At 6 h, α1-β1 subunits were colocalized 1.3 fold more on TiN_xO_y hence suggesting more interactions (figure 3 E). Note that some clusters—visible as little yellow dots on the cells' periphery—were present only on cells grown on TiN_xO_y and not on Ti-SLA (figure 3 A4, B4). The difference in colocalization was no longer significant at 24 h at which time some clusters appeared on cells grown on Ti-SLA, although still more were found on TiN_xO_y (figure 3 E, C4, D4). For α2-β1, the colocalization coefficient was equal at 6 h, and increased by 1.3 times on TiN_xO_y after 24 h (figure 4 E). Some clusters in close vicinity to nuclei were more visible at 6 h on TiN_xO_y when compared to Ti-SLA (figure 4 A4, B4); after 24 h, the clusters were distributed on the whole cell surface but to a greater extent on TiN_xO_y (figure 4 C4, D4).

Focal adhesions were analyzed by scrutinizing ITGβ1 colocalization with vinculin and paxillin (figures 5–6). There was no difference in terms of fluorescence intensity for vinculin, either at 6 or 24 h (figure 5 E, A3, B3, C3, D3). However, the colocalization β1-vinculin was markedly more pronounced (three times) and homogeneously distributed on the surface of cells grown on TiN_xO_y as compared to Ti-SLA at 6 h. Only few focal points (yellow clusters) could be detected at that time on either surface (figure 5 E, A4, B4). After 24 h, ITGβ1 and vinculin were equally colocalized (figure 5 E) in a multitude of sites on the cells' periphery; note that the cells were indeed largely more spread on TiN_xO_y (figure 5 C4, D4). Some focal adhesions were also observable as red

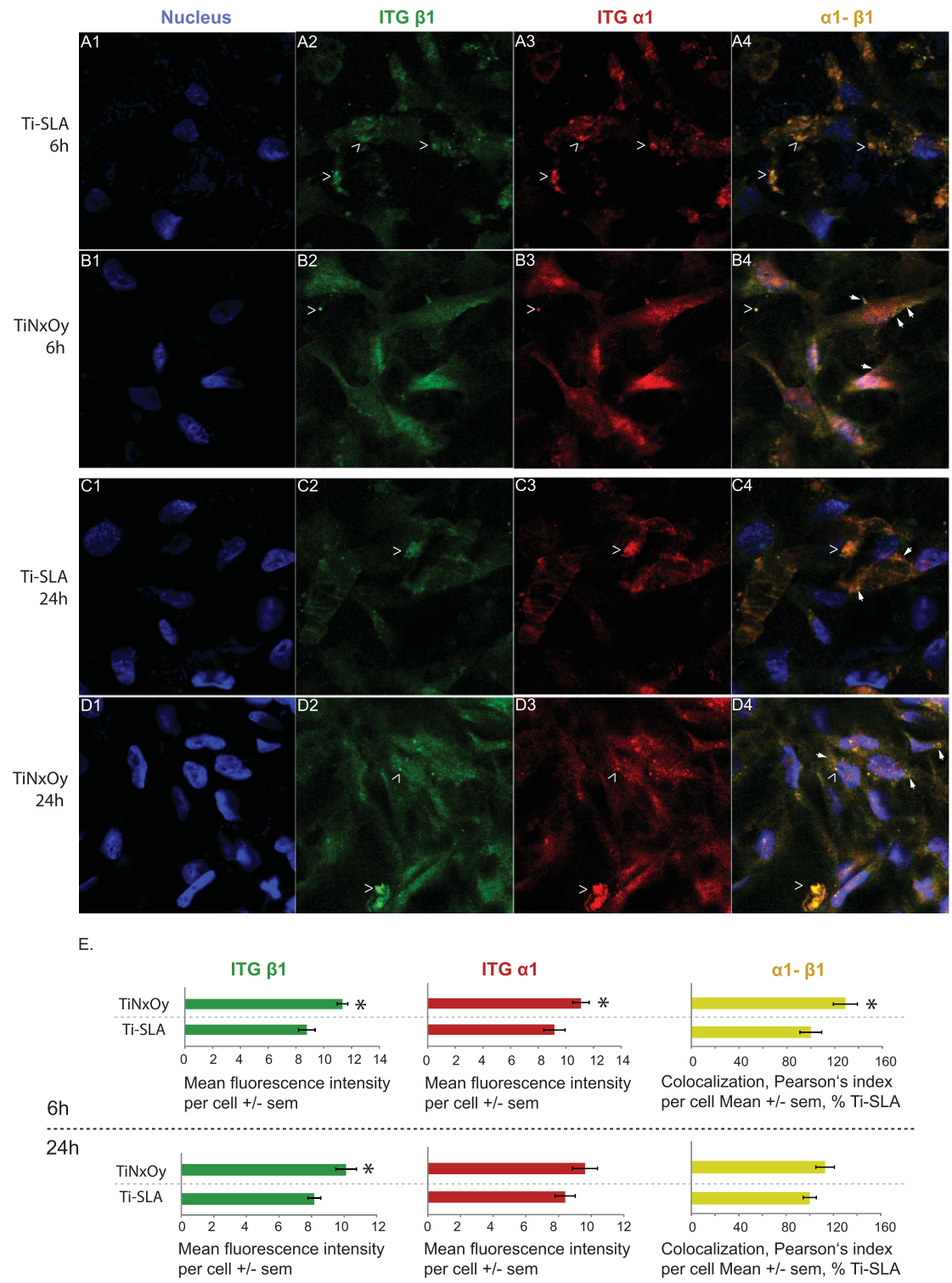

Figure 3. Typical immunostainings (ITGα1 and β1) of HOS grown on Ti-SLA (6 h: A1–4; 24 h: C1–4) and TiN_xO_y (6 h: B1–4; 24 h: D1–4) plates. Blue, nuclei; green, integrin β1; red, integrin α1; yellow (merged green + red), integrin α1-β1. White caret: examples of artifacts or saturated areas caused by the surface reliefs, excluded from computations; white arrows: examples of α1-β1 colocalization clusters. The fluorescence intensities for each channel (E) were calculated per cell and expressed as mean +/− sem; three separate experiments in duplicate (18 plates for ITG β1, 2–20 cells/section; six plates for ITG α1, 1–18 cells/section). The Pearson's correlation index (E) was calculated to assess for α1-β1 colocalization (expressed as percent of Ti-SLA at 6 h or 24 h, mean +/− sem).*: $p < 0.05$.

clusters (no colocalization β1-vinculin), suggesting the implication of other ITGβ subunits in the initial mechanisms of cell adhesion and spreading (figure 5 C4, D4). The same staining procedures were also conducted on human primary osteoblasts at 6 and 24 h and demonstrated a similar pattern to that of HOS cells in terms of expression-colocalization of β1-vinculin (figure 5 A5, B5, C5, D5).

As shown in figure 6 (E, A3, B3, C3, D3), paxillin expression was not modified at 6 and 24 h, despite a

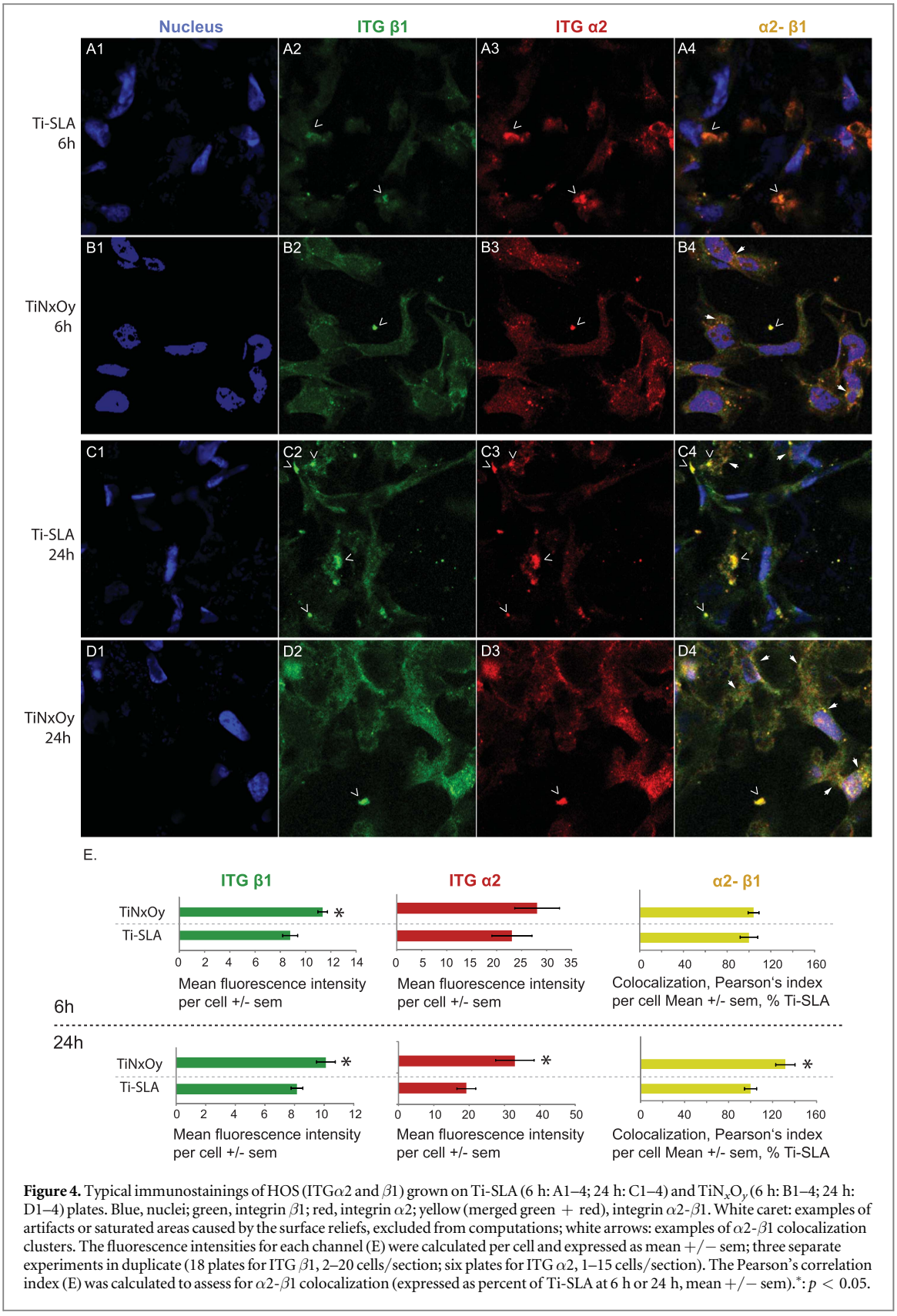

Figure 4. Typical immunostainings of HOS (ITGα2 and β1) grown on Ti-SLA (6 h: A1–4; 24 h: C1–4) and TiN_xO_y (6 h: B1–4; 24 h: D1–4) plates. Blue, nuclei; green, integrin β1; red, integrin α2; yellow (merged green + red), integrin α2-β1. White caret: examples of artifacts or saturated areas caused by the surface reliefs, excluded from computations; white arrows: examples of α2-β1 colocalization clusters. The fluorescence intensities for each channel (E) were calculated per cell and expressed as mean +/− sem; three separate experiments in duplicate (18 plates for ITG β1, 2–20 cells/section; six plates for ITG α2, 1–15 cells/section). The Pearson's correlation index (E) was calculated to assess for α2-β1 colocalization (expressed as percent of Ti-SLA at 6 h or 24 h, mean +/− sem).*: $p < 0.05$.

slight tendency for overexpression on TiN_xO_y at 24 h when compared to Ti-SLA. Six hours after seeding, no difference regarding the colocalization of ITGβ1 and paxillin was observable. Most of these interactions were encountered in the vicinity of the nuclei on both surfaces (figure 6 A4, B4). This profile was almost the same after 24 h on Ti-SLA (figure 6 C4), while many focal points β1-paxillin were visible on the periphery of cells grown on TiN_xO_y (figure 6 D4), combined to a ~1.3 times increase (significant) in colocalization (figure 6 E). Again, some focal points (red) not involving ITGβ1 were present. Repeating the procedure on

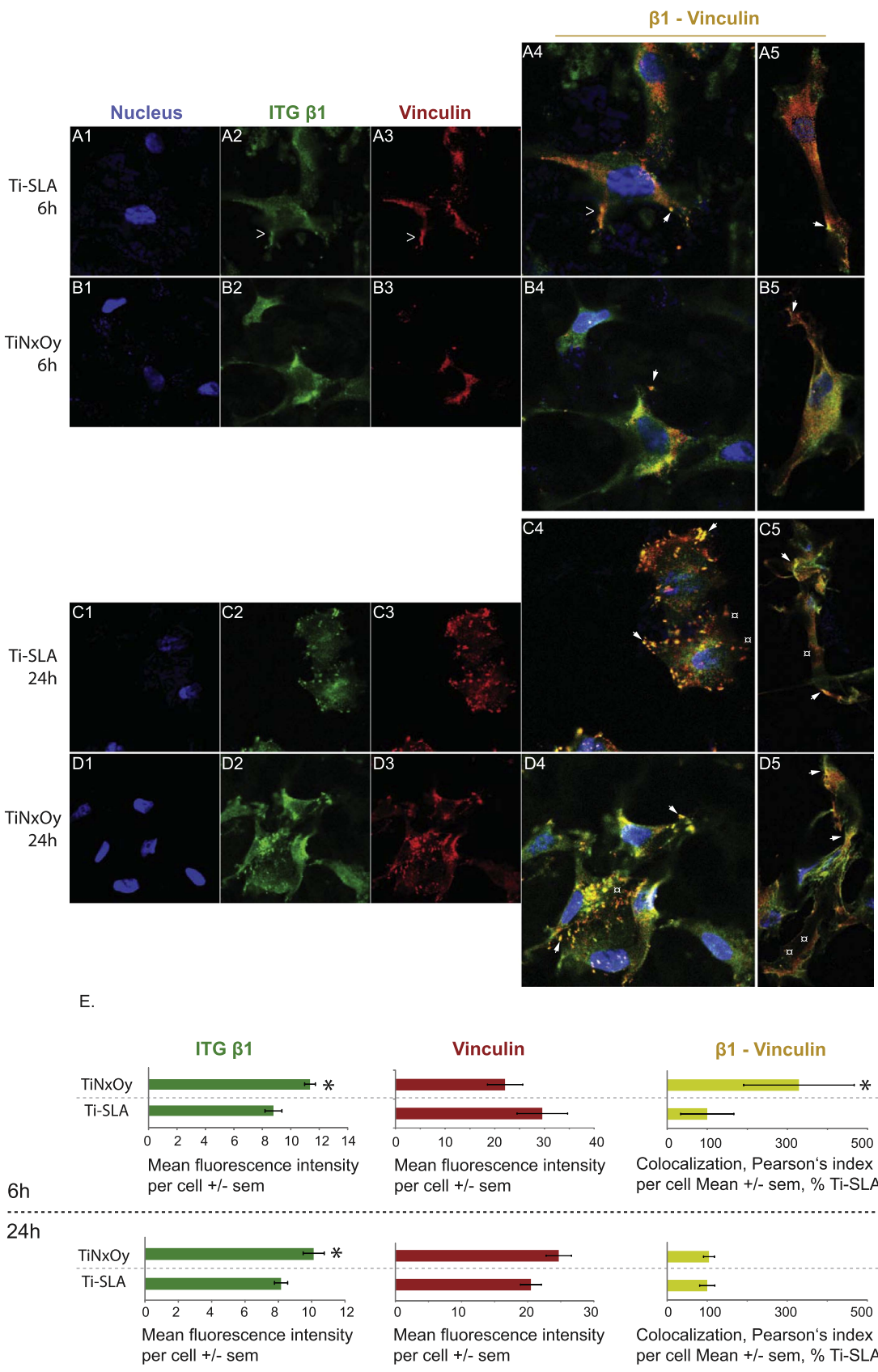

Figure 5. Typical immunostainings (ITGβ1 and vinculin) of osteoblasts (HOS and primary osteoblasts (hOBs)) grown on Ti-SLA (6 h: HOS A1–4, hOBs A5 ; 24 h: HOS C1–4, hOBs C5) and TiN_xO_y (6 h: HOS B1–4, hOBs B5; 24 h: HOS D1–4, hOBs D5) plates. Blue, nuclei; green, integrin β1; red, vinculin; yellow (merged green + red), integrin β1-vinculin. White caret: examples of artifacts or saturated areas caused by the surface reliefs, excluded from computations; white arrows: examples of β1-vinculin colocalization clusters (focal adhesions); white circle-cross: example of focal adhesion clusters where vinculin is involved and ITGβ1 is not. The fluorescence intensities (E) for each channel were calculated per cell and expressed as mean +/− sem; three separate experiments in duplicate (18 plates for ITG β1, 2–20 cells/section; six plates for vinculin, 1–16 cells/section). The Pearson's correlation index (E) was calculated to assess for β1-vinculin colocalization (expressed as percent of Ti-SLA at 6 h or 24 h, mean +/− sem). *: $p < 0.05$.

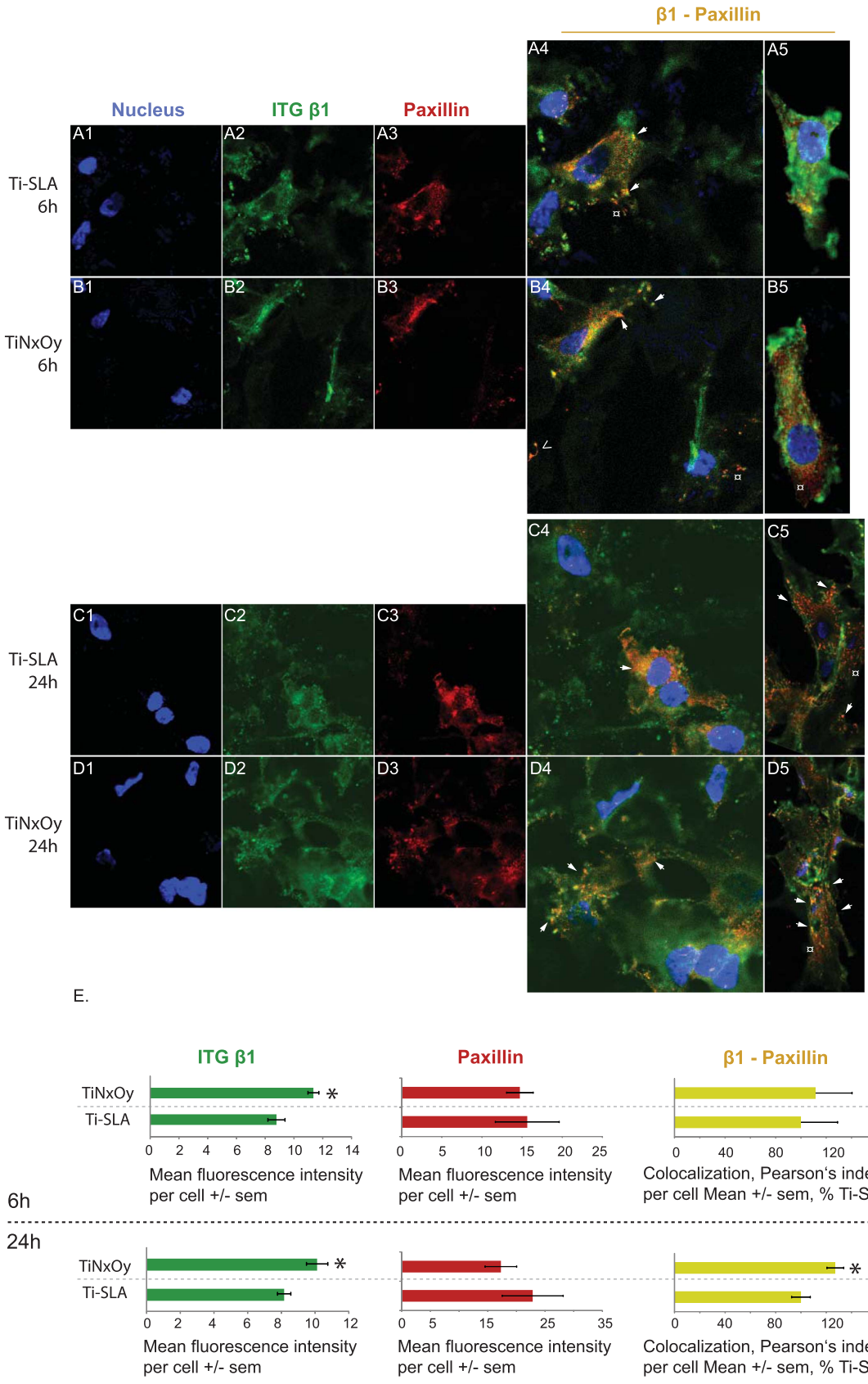

Figure 6. Typical immunostainings (ITGβ1 and paxillin) of osteoblasts (HOS and primary osteoblasts (hOBs)) grown on Ti-SLA (6 h: HOS A1–4, hOBs A5 ; 24 h: HOS C1–4, hOBs C5) and TiN_xO_y (6 h: HOS B1–4, hOBs B5; 24 h: HOS D1–4, hOBs D5) plates. Blue, nuclei; green, integrin β1; red, paxillin; yellow (merged green +red), integrin β1-paxillin. White caret: examples of artifacts or saturated areas caused by the surface reliefs, excluded from computations; white arrows: examples of β1-vinculin colocalization clusters (focal adhesions); white circle-cross: example of focal adhesion clusters where paxillin is involved and ITGβ1 is not. The fluorescence intensities (E) for each channel were calculated per cell and expressed as mean +/− sem; three separate experiments in duplicate (18 plates for ITG β1, 2–20 cells/section; 6 plates for paxillin, 1–14 cells/section). The Pearson's correlation index (E) was calculated to assess for β1-paxillin colocalization (expressed as percent of Ti-SLA at 6 h or 24 h, mean +/− sem). *: $p < 0.05$.

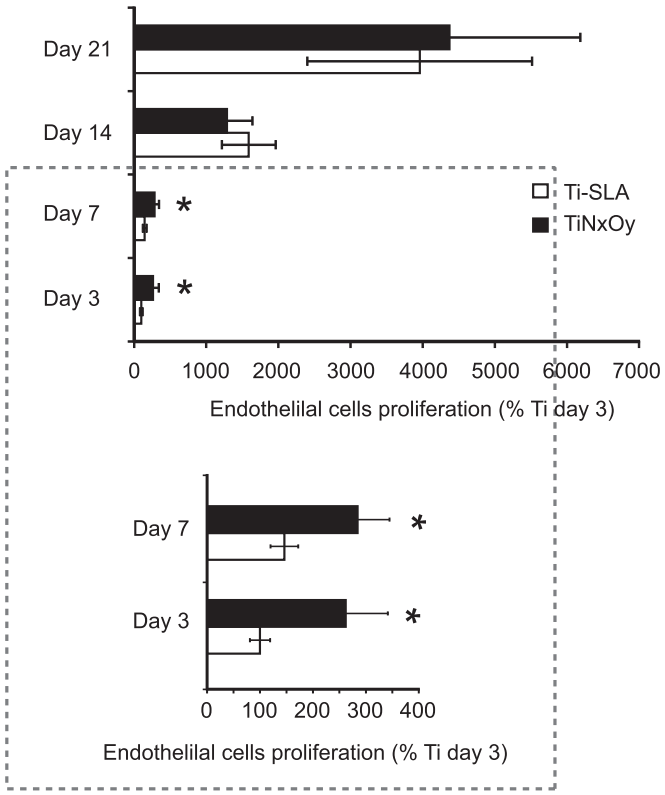

Figure 7. Endothelial cells proliferation from days 3 to 21 on Ti-SLA (white bars) and TiN_xO_y (black bars). Day 3 and day 7 were represented with a smaller scale on the lower panel. ($n = 9$, % Ti-SLA at day 3, mean +/− sem). *: $p < 0.05$.

human primary osteoblasts duplicated and thus confirmed the results presented above (figure 6 A5, B5, C5, D5).

Endothelial cell proliferation

Osseointegration is a multicellular process, in which endothelial cells support blood vessel formation and hence play a major role. Three sets of experiments were conducted with human endothelial cells alone or in co-culture with HOS cells. The human umbilical cell line EAhy926 (EA) was used.

In a first set of experiments, the effect of bare Ti-SLA and TiN_xO_y coatings on EA cell proliferation was compared over a period of 21 days. As shown in figure 7, the proliferation of EA cells on TiN_xO_y was increased by 2.5 times during the first week after seeding. No difference though, was observable after one week.

Cocultures osteoblasts—endothelial cells

In another set of experiments, we colcultured EA and HOS cells on Ti-SLA and TiN_xO_y. The aim was to investigate the effect of a direct HOS-EA contact on the cells' survival and proliferation. A 5/1 EA-HOS ratio was used for seeding. After 1, 3, 6 and 8 days, the cells were detached and immunostained with an anti-CD31 expressed on EA membranes and not on HOS. The cells were then analyzed by flow cytometry and discriminated according to their CD31 expression. Eventually their respective proportions were calculated. As shown in figure 8 (G), the EA proportion decreased to a total of about 20% on both surfaces, without any notable difference. Consequently, by mirror effect, the HOS proportion increased to about 80% of the total, on both surfaces and without difference (figure 8 (H)).

Cell to cell communication

A last set of experiments was designed to assess the mechanisms by which HOS cells in the early period after adhesion, possibly modulated their own proliferation and migration as well as that of the EA cells, via the release of soluble factors. A wound assay was conducted on confluent EA and HOS cultures. The covering of the wound stripe was assessed after it was exposed to the media obtained from HOS cells grown for 1 day either on Ti-SLA or on TiN_xO_y. As shown in figure 9(A), at day 1, EA cells recovered about 65% of the wound when they were cultured with a medium from HOS grown on Ti-SLA while a 85% recovery was observed with media from TiN_xO_y. In both instances, the wound was largely filled by a dense cell layer after two days. When the wound was created on an HOS cell layer, no substantial difference was observable as the scratched stripe was already largely covered at day 1 in both instances (figure 9(B)). However, the layer that grew with Ti-SLA-HOS conditioned medium appeared less dense in comparison with the layer

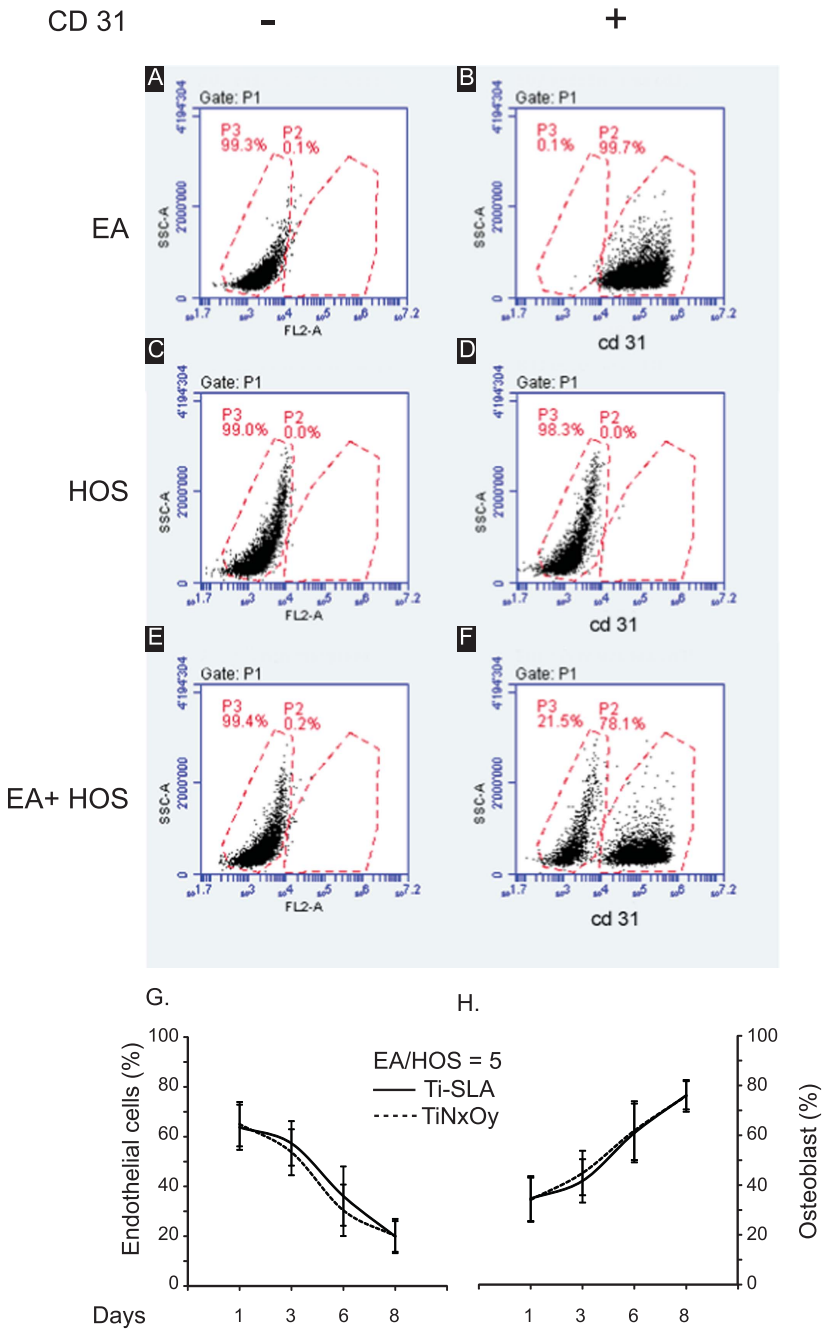

Figure 8. Proportion of endothelial cells (EA) and osteoblasts (HOS) in cocultures on Ti-SLA and TiN_xO_y from day 1 to 8. Typical plots obtained by flow cytometry with EA (A), (B), HOS (C), (D) and EA + HOS (E), (F) (gated on living cells (P1); P3: CD31 negative cells, P2: CD31 positive cells). Relative proportions of EA and HOS were calculated from these plots, with an initial ratio EA/HOS = 5 (G), (H). Dark line: Ti-SLA, dashed line: TiN_xO_y ($n = 9$, mean +/− sem).

grown with TiN_xO_y-HOS medium. About 10% of the surface was left uncovered with Ti-SLA-HOS medium versus 3% for TiN_xO_y-HOS. There were no observable differences at day 2.

Modulation of inflammation

Finally, we aimed at analyzing the capacity of HOS cells to modulate inflammation by producing cytokines. To this end, the gene expression of some cytokines was analyzed. HOS cells were grown either on Ti-SLA or TiN_xO_y for 3 days. RT-PCR analyses were performed at day 1 to day 3 (table 1). They revealed a net decrease of IL8 and IL-11 on TiN_xO_y at day 1 when compared to Ti-SLA. Only at day 3 did HOS cells on Ti-SLA reach the low level of expression observed on TiN_xO_y at day 1. For IL-6, no significant difference was observed between Ti-SLA and TiN_xO_y at day 1 and 3, except for a slight decrease at day 3 on both surfaces. IL-10 expression was not significantly different on both surfaces at day 1 and 3 but a tendency to the decrease was recorded on Ti-SLA when the expression remained stable on TiN_xO_y.

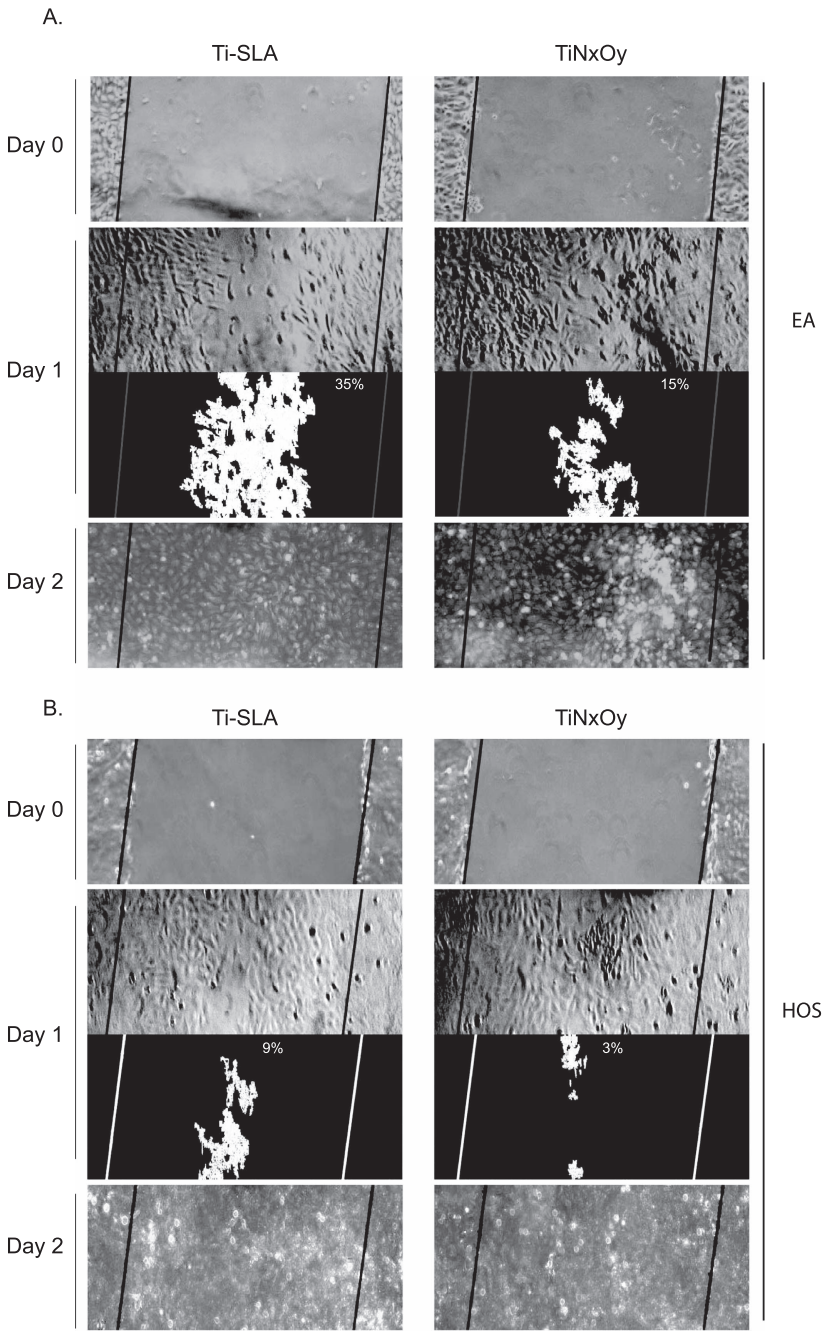

Figure 9. Effect of conditioned media (conditioned by HOS grown on Ti-SLA or TiN_xO_y for one day) on the migration of EA or HOS. Cells plated on polystyrene dishes were cultured until they reached confluence. The wound was then performed and the cells were exposed to conditioned media. Representative views of EA (A) and HOS (B) wound assay from day 0 to day 2. At day 1, the cell layer was digitally extracted to visualize easily the area that remained uncovered within the wound. The percentage represent proportion of uncovered area versus total wound area. One representative experiment out of three realized in triplicate.

Discussion

The present project was designed to investigate the mechanisms of osteoblast adhesion on microrough titanium and especially on TiN_xO_y coatings taken as catalysts for cell adherence, spreading and proliferation. The expression of integrins, their location, activation and implication in focal adhesion were analyzed. Through a set of pilot experiments aimed at elucidating the relation between bone-, inflammatory- and endothelial cells on these films, an overview of the osseointegrative process on TiN_xO_y was developed and is presented below.

In contrast to our previous studies where we used primary human osteoblasts, the present study was essentially conducted with the 'osteoblast-like' cells HOS. The HOS line was originally isolated from a human osteosarcoma and is now an established model for *in vitro* studies [24]. We used these cells primarily due to their availability. In effect, the immunostainings and mRNA extractions requested large amounts of cells—quantities that primary osteoblasts from the

Table 1. Interleukines gene expression of HOS on Ti-SLA and TiN_xO_y at day 1–3.

Cytokines	Day 1		Day 3	
	Ti-SLA	TiN_xO_y	Ti-SLA	TiN_xO_y
IL-8	1	$0.31 \pm 0.09^*$	0.46 ± 0.3	0.25 ± 0.12
IL-11	1	$0.57 \pm 0.17^*$	0.27 ± 0.06	0.28 ± 0.1
IL-6	1	0.94 ± 0.05	0.78 ± 0.1	0.88 ± 0.09
IL-10	1	0.91 ± 0.13	0.79 ± 0.04	0.93 ± 0.05

% Ti-SLA at day 1, mean $\pm$ SEM, $n = 6$. $^*p < 0.05$ as compared to Ti-SLA at the same day.

same lineage would be unable to provide. The prerequisites for the choice of the HOS line was that it duplicated the data obtained with primary osteoblasts grown on TiN_xO_y versus Ti-SLA, that is, (i) a 50% increase in proliferation and (ii) the preservation of a high level of differentiation [5]. HOS cells met these requirements on the basis of reasazurin assays and gene expression analyses (figure 1) and were therefore chosen as model for the entire study. MG63 is another osteoblastic cell line commonly used in studies on bone metabolism. MG63 also satisfied our requirements (data not shown), but the cells' proliferation was too rapid under our conditions (especially for adhesion assays) and therefore they were excluded from this study. Still, recognizing the superiority of primary cells for *in vitro* testing we conducted assessment verifications with primary cells, especially during the identification of focal adhesions.

Finally, the endothelial cell line Eahy926 that was used in a series of assays is a standard model for *in vitro* testing [25]. These cells are issued from the fusion of primary human umbilical vein endothelial cells with the human pulmonary adenocarcinoma A549.

In a recent study, we observed that cells grown on TiN_xO_y spread faster than cells grown on Ti-SLA very early after contacting the surfaces [8]. Except for cell density, no further difference between surfaces could be detected after 3 days. Therefore we hypothesized that the cells grown on TiN_xO_y behaved similarly to those grown on Ti-SLA, but initiate their proliferation and migration faster. The important effects observed at day 7 may merely result from improved mechanisms of adhesion [5, 7, 8]. To verify this hypothesis, we analyzed the adhesion of HOS cells at 6 and 24 h after seeding. Focusing on differential integrin expression in the HOS lineage at day 1, we observed a net increase for ITGβ1, α1 and α2 on TiN_xO_y when compared to Ti-SLA. ITGβ1 has a pivotal role in osteoblast adhesion on rough titanium [13] while α1 and α2 are also known as key players, mainly in spreading, maturation and differentiation processes [12, 26]. Still, their potential involvement in adherence mechanisms is unknown. After 6 h, we confirmed that ITGβ1 was markedly more expressed on HOS membranes when the cells were grown on TiN_xO_y. ITGβ1 was also more recruited in newly engaged focal adhesion clusters on TiN_xO_y, as shown by higher vinculin colocalisations when compared to Ti-SLA. After 24 h, not only were the focal adhesions involving β1 more numerous on TiN_xO_y but also more active. In effect, Paxillin that succeeds vinculin in the recruitment process for focal adhesion activation [27] was markedly more colocalized on TiN_xO_y cells when compared to those grown on Ti-SLA. Regarding the dimer associated to ITGβ1 in these adhesions, there was clear evidence that α1 was more expressed and more colocalized to β1 on TiN_xO_y at 6 h and then replaced by α2 at 24 h.

To summarize, the initial cell attachment (at 6 h) most likely is mediated by ITGβ1, probably associated to ITGα1. The engagement of these integrins (ITGβ1) in focal adhesions is proven by their clustering with vinculin. These mechanisms are observed on both surfaces but are more pronounced on TiN_xO_y than on Ti-SLA. After 24 h, the engagement of β1 in focal adhesions is more advanced, as shown by the recruitment of paxillin. The cell spreading that follows initial cell adherence could be facilitated by α2-β1 on TiN_xO_y.

ITG α1-β1 and ITG α2-β1 are receptors for collagen 1 [10]. Their expression is stable at 24 h either on Ti-SLA or TiN_xO_y. Our results thus suggest that collagen is of prime importance in cell adhesion and migration on implant surfaces, and especially on TiN_xO_y coatings.

In addition to collagen, FN is another important component of the ECM and is stably expressed in hOBs grown on TiN_xO_y, whereas it is lessened on Ti-SLA from day 1 to day 3. The dimer α5-β1, a receptor for FN, [10] was described as mediating adhesion and proliferation in osteoblasts starting from day 3 [16]. In our conditions, α5 was stably expressed at day 1, and indeed overexpressed on TiN_xO_y versus Ti-SLA at day 3, but very slightly. Therefore, based on gene expression, if we could not rule out α5-β1's involvement in HOS cell adhesion on microrough titanium at day 1 (the gene is expressed), it does not, however, contribute to facilitating the processes observed on TiN_xO_y as compared to Ti-SLA. On the other hand, the overexpression of ITG α5-β1 from day 3 on may explain a faster initiation of proliferation. Further analyses will be needed since we did not perform co-stainings in first intention. In addition to α5, some other α subunits are expressed in osteoblasts (namely α3, α6 and αv) and can dimerize with β1. Still, as none

of these associations was described on titanium, they were not investigated further.

Finally, ITG αv-β3 is another receptor for FN. ITGβ3 dimerizes solely with αv [10]. The two subunits are expressed equally on Ti-SLA and TiN_xO_y. We noticed at day 1 that vinculin and paxillin were implied in focal adhesions in which ITGβ1 was not detected. ITGβ3 therefore may be an ideal candidate as a partner in these sites. Future experiments with the aim of identifying a possible implication of αvβ3 in the early adhesion of osteoblast on microrough titanium may be of interest, although a recent study only found a minor implication of αv in osteoblasts grown on Ti [13]. In conclusion, gene expression at day 1 does not plead for an implication of this dimer in the benefic effects of TiN_xO_y.

Except from gene expression analysis, we did not pursue the study of adhesion mechanisms beyond day 3. Due to the large cell density, many cells overlapped causing additive fluorescent signals that hampered interpretation—note that this effect was added to a surface topography that was unfavorable for such analyses from the onset. Regarding gene expression, we observed that ITGα1 and α2 were no longer overexpressed on TiN_xO_y versus Ti-SLA, in contrast to ITGβ3, α5 and αv. As to ITGβ1, it was still largely overexpressed on TiN_xO_y. It therefore follows that the FN receptors α5-β1 and αv-β3 may be overexpressed and active on TiN_xO_y coatings with respect to Ti-SLA as well. This hypothesis is reinforced by the observation that HOS cells produced more FN on TiN_xO_y.

Finally, an explanation for the mechanisms of facilitated adhesion of HOS cells on TiN_xO_y coatings could be (i) an improvement of cell adhesion on collagen via α1-β1 and α2-β1—the accelerated cell spreading of the osteoblasts on TiN_xO_y [8] would be due specifically to α2-β1 and, (ii) an initiation of the proliferation eased by FN and α5-β1 and αv-β3 once the adhesion is completed.

Osseointegration is a complex process that requires the collaboration of several cell types. Neutrophils, mesenchymal stem cells, osteoblasts, endothelial cells and osteoclasts communicate via direct contacts or secretion of soluble factors [9]. For instance, endothelial cells are capable of producing BMP2 and thus stimulate osteoblast proliferation and differentiation [17–19]. Conversely osteoblasts can produce growth factors such as VEGF which will stimulate endothelial cell proliferation, migration and differentiation [20–22]. Osteoblasts also secrete some pro- and anti-inflammatory cytokines so they can modulate the inflammatory response from inside the integration interface [28]. In this context, we were interested in the relation between osteoblasts and endothelial cells with the aim of evaluating the effects of TiN_xO_y in this interaction.

We first demonstrated that endothelial cells may also benefit of a direct contact with TiN_xO_y since their proliferation is increased during the first week. In this regard, TiN_xO_y surfaces have primarily found acceptance in cardiovascular (i.e. stent) applications as they largely prevent restenosis [29, 30] and improve endothelial regeneration [31]. The exact mechanism by which TiN_xO_y becomes active has not been elucidated even if it was reasoned that the films would somehow counteract the inflammatory process [32, 33]. In the present report, we provide an element of response by demonstrating that TiN_xO_y coatings may promote endothelial cell proliferation and thus improve endothelial regeneration in endosseous- as well as in cardiovascular applications.

We also wondered whether a direct contact between osteoblasts and endothelial cells would affect the survival- and proliferation rate of both cells in coculture on Ti-SLA or TiN_xO_y. We used a ratio of 5/1 (EA/HOS) that is described to allow a cell contact during a 1 week experiment [34]. We could not provide evidence that a physical contact improves the survival of the endothelial cells over a period of 1 week—whether the cells were grown on Ti-SLA or on TiN_xO_y. Osteoblasts also were not impacted regarding their proliferation. However, in a recent study, it was shown that a coculture of Ob and EA cells affected the angiogenic potential of the EA lineage [35]. Their production of angiogenic factors such as vWF, thrombomdulin, E selectin or VEGF varied with the microroughness and the degree of hydrophilicity of the surface. As we have now developed and control the coculture model, it will therefore be of great interest to analyze the differentiation of the EA cells in detail when they are grown alone, on TiN_xO_y or in coculture with osteoblasts.

Regarding soluble factors and cell communications, our work on conditioned media with HOS grown on Ti-SLA or TiN_xO_y for 1 day demonstrated that a single day of contact with TiN_xO_y suffices for osteoblasts to produce and secrete factors capable of stimulating endothelial cell migration (as well as their own, but to a lesser extent). It is known that osteoblasts secrete growth factors such as VEGF, EGF or FGF when they are grown on microrough titanium [36]. Hence they appear as prime candidates when searching for an explanation as to how HOS cells would increase the migration of EA cells after only one day of culture. Whether TiN_xO_y also modulates the production of these factors remains to be assessed.

Osseointegration implies a moderate and well coordinated inflammatory process [9]. Osteoblasts grown on microrough titanium, can modulate the inflammatory response, especially via a decrease in the production of proinflammatory cytokines such as IL-6 or IL-8, in parallel with an increase of anti-inflammatory cytokines such as IL-10 [28]. Hence, IL-6 functions as an activator of oscteoclasts [37], similar to the cytokine IL-11 which also promotes the degradation of collagen 1 [38, 39]. As for IL-8, IL-11 is a potent chemoattractant for neutrophils [40] while IL-10 blocks the production of proinflammatory cytokines [41]. In the present work, we demonstrate that HOS cells

express 2- to 3 times less IL-11 and IL-8 at day 1 when they had been in contact with TiN_xO_y (i.e. at day 1) (as opposed to Ti-SLA). After 3 days, the cytokines levels were equivalent on both surfaces. By maintaining an osteoblastic cytokine production as low as on Ti-SLA nay weaker, TiN_xO_y permits a modulation of the inflammatory response driven by osteoblast and the development of a favorable environment for bone regeneration. These observations match those obtained with 'SLActive', a hydrophilic and micro-rough surface treatment [28] also known for its improvements of early osseointegration [42] in equivalent amounts to TiN_xO_y [6].

Altogether, these results demonstrate that TiN_xO_y coatings facilitate osteoblast adhesion and spreading when compared to the microrough standard SLA. The integrin $\beta1$, associated to $\alpha1$ and $\alpha2$ subunits plays a central role in these mechanisms. In the early days after initial cell contact, integrins αv-$\beta3$ and $\alpha5$-$\beta1$ take over and accelerate the proliferation of osteoblasts on TiN_xO_y films. As such, it appears that the osteoblasts' affinity for collagen 1 (ITG $\alpha1$-$\beta1$/$\alpha2$-$\beta1$ ligand) first and later for FN (ITG $\alpha5$-$\beta1$/αv-$\beta3$ ligand) is augmented when cells are grown on TiN_xO_y as compared to Ti-SLA.

Beyond the specific effects of TiN_xO_y versus Ti-SLA, the present work offers a broader perspective as it points out the importance of integrins $\alpha1$-$\beta1$ and $\alpha2$-$\beta1$ in osteoblast adhesion on microrough titanium—a surface structure that was hitherto primarily known for its role in osteoblast maturation and differentiation.

In conclusion, TiN_xO_y coatings optimize the process of osseointegration at several levels, that is, (i) on osteoblast adhesion and proliferation, (ii) by supporting neovascularization and (iii) by fostering the development of a suitable inflammatory environment. Obviously, further work is needed, most particularly to complete our knowledge of the mechanisms of adhesion on TiN_xO_y and to confirm the impact of these coatings on neovascularization. Still, the general pattern that emerges from these studies indicates that the effect of TiN_xO_y on osseointegration is global and not merely targeted towards a specific cell population.

Acknowledgments

The assistance of Ms Patricia Vasquez-Pico and Ms Calderin-Sollet in the development of immunostaings is gratefully acknowledged. We are also indebted to thank Mr Fabrice Bisoffi for his help in deposition of coatings. The study was supported by grants CR32I2_137739 and CR32I2_156295 from the Swiss National Science Foundation.

References

[1] Bachle M and Kohal R J 2004 A systematic review of the influence of different titanium surfaces on proliferation, differentiation and protein synthesis of osteoblast-like MG63 cells *Clin. Oral Implants Res.* **15** 683–92

[2] Buser D, Schenk R K, Steinemann S, Fiorellini J P, Fox C H and Stich H 1991 Influence of surface characteristics on bone integration of titanium implants. A histomorphometric study in miniature pigs *J. Biomed. Mater. Res.* **25** 889–902

[3] Le Guehennec L, Soueidan A, Layrolle P and Amouriq Y 2007 Surface treatments of titanium dental implants for rapid osseointegration *Dental Mater.* **23** 844–54

[4] Parekh R B, Shetty O and Tabassum R 2012 Surface modifications for endosseous dental implants *Int. J. Oral Implantol.Clin. Res.* **3** 116–21

[5] Durual S, Pernet F, Rieder P, Mekki M, Cattani-Lorente M and Wiskott H W 2011 Titanium nitride oxide coating on rough titanium stimulates the proliferation of human primary osteoblasts *Clin. Oral Implants Res.* **22** 552–9

[6] Durual S *et al* 2013 $TiNO_x$ coatings on roughened titanium and CoCr alloy accelerate early osseointegration of dental implants in minipigs *Bone* **52** 230–7

[7] Rieder P, Scherrer S, Filieri A, Wiskott H W and Durual S 2012 $TiNO_x$ coatings increase human primary osteoblasts proliferation independently of the substrate: a short report *Biomed. Mater. Eng.* **22** 277–81

[8] Moussa M *et al* 2016 Modulation of osteoblast behavior on TiN_xO_y coatings by altering the N/O stoichiometry while maintaining a high thrombogenic potential *J. Biomater. Appl.* **30** 1219–29

[9] Gittens R A, Olivares-Navarrete R, Schwartz Z and Boyan B D 2014 Implant osseointegration and the role of microroughness and nanostructures: lessons for spine implants *Acta Biomater.* **10** 3363–71

[10] Srichai M B and Zent R 2010 Integrin structure and function *Cell-Extracellular Matrix Interactions in Cancer* ed R Zent and A Pozzi (Berlin: Springer)

[11] Boyan B D, Cheng A, Olivares-Navarrete R and Schwartz Z 2016 Implant surface design regulates mesenchymal stem cell differentiation and maturation *Adv. Dental Res.* **28** 10–7

[12] Olivares-Navarrete R *et al* 2008 Integrin alpha2beta1 plays a critical role in osteoblast response to micron-scale surface structure and surface energy of titanium substrates *Proc. Natl Acad. Sci. USA* **105** 15767–72

[13] Olivares-Navarrete R *et al* 2015 Role of integrin subunits in mesenchymal stem cell differentiation and osteoblast maturation on graphitic carbon-coated microstructured surfaces *Biomaterials* **51** 69–79

[14] Heino J 2000 The collagen receptor integrins have distinct ligand recognition and signaling functions *Matrix Biol.* **19** 319–23

[15] Pozzi A, Wary K K, Giancotti F G and Gardner H A 1998 Integrin alpha1beta1 mediates a unique collagen-dependent proliferation pathway *in vivo J. Cell Biol.* **142** 587–94

[16] Keselowsky B G, Wang L, Schwartz Z, Garcia A J and Boyan B D 2007 Integrin alpha(5) controls osteoblastic proliferation and differentiation responses to titanium substrates presenting different roughness characteristics in a roughness independent manner *J. Biomed. Mater. Res.* A **80** 700–10

[17] Bouletreau P J *et al* 2002 Hypoxia and VEGF up-regulate BMP-2 mRNA and protein expression in microvascular endothelial cells: implications for fracture healing *Plast Reconstr. Surg.* **109** 2384–97

[18] Fiedler J, Brill C, Blum W F and Brenner R E 2006 IGF-I and IGF-II stimulate directed cell migration of bone-marrow-derived human mesenchymal progenitor cells *Biochem. Biophys. Res. Commun.* **345** 1177–83

[19] Veillette C J and von Schroeder H P 2004 Endothelin-1 down-regulates the expression of vascular endothelial growth factor-A associated with osteoprogenitor proliferation and differentiation *Bone* **34** 288–96

[20] Clarkin C E, Emery R J, Pitsillides A A and Wheeler-Jones C P 2008 Evaluation of VEGF-mediated signaling in primary human cells reveals a paracrine action for VEGF in osteoblast-mediated crosstalk to endothelial cells *J. Cell Physiol.* **214** 537–44

[21] Clarkin C E, Garonna E, Pitsillides A A and Wheeler-Jones C P 2008 Heterotypic contact reveals a COX-2-mediated suppression of osteoblast differentiation by endothelial cells: a negative modulatory role for prostanoids in VEGF-mediated cell: cell communication? *Exp. Cell Res.* **314** 3152–61
[22] Kaigler D, Wang Z, Horger K, Mooney D J and Krebsbach P H 2006 VEGF scaffolds enhance angiogenesis and bone regeneration in irradiated osseous defects *J. Bone Miner. Res.* **21** 735–44
[23] Banakh O *et al* 2014 Sputtered titanium oxynitride coatings for endosseous applications: physical and chemical evaluation and first bioactivity assays *Appl. Surf. Sci.* **317** 986–93
[24] Mohseny A B *et al* 2011 Functional characterization of osteosarcoma cell lines provides representative models to study the human disease *Lab Invest.* **91** 1195–205
[25] Unger R E, Krump-Konvalinkova V, Peters K and Kirkpatrick C J 2002 *In vitro* expression of the endothelial phenotype: comparative study of primary isolated cells and cell lines, including the novel cell line HPMEC-ST1.6R *Microvasc. Res.* **64** 384–97
[26] Rosa A L *et al* 2014 Nanotopography drives stem cell fate toward osteoblast differentiation through alpha1beta1 integrin signaling pathway *J. Cell Biochem.* **115** 540–8
[27] Humphries J D, Wang P, Streuli C, Geiger B, Humphries M J and Ballestrem C 2007 Vinculin controls focal adhesion formation by direct interactions with talin and actin *J. Cell Biol.* **179** 1043–57
[28] Hyzy S L, Olivares-Navarrete R, Hutton D L, Tan C, Boyan B D and Schwartz Z 2013 Microstructured titanium regulates interleukin production by osteoblasts, an effect modulated by exogenous BMP-2 *Acta Biomater.* **9** 5821–9
[29] Windecker S, Billinger M and Hess O 2006 Stent coating with titanium-nitride-oxide for prevention of restenosis *Eurointervention* **2** 146–8
[30] Windecker S *et al* 2001 Stent coating with titanium-nitride-oxide for reduction of neointimal hyperplasia *Circulation* **104** 928–33
[31] Annala A P, Lehtinen T, Kiviniemi T O, Ylitalo A, Nammas W and Karjalainen P P 2013 Vascular healing early after titanium-nitride-oxide-coated stent implantation assessed by optical coherence tomography *J. Invasive Cardiol.* **25** 186–9 PMID: 23549492
[32] Garg U C and Hassid A 1989 Nitric oxide-generating vasodilators and 8-bromo-cyclic guanosine monophosphate inhibit mitogenesis and proliferation of cultured rat vascular smooth muscle cells *J. Clin. Invest.* **83** 1774–7
[33] Mooradian D L, Hutsell T C and Keefer L K 1995 Nitric oxide (NO) donor molecules: effect of NO release rate on vascular smooth muscle cell proliferation *in vitro J. Cardiovasc. Pharmacol.* **25** 674–8
[34] An N, Schedle A, Wieland M, Andrukhov O, Matejka M and Rausch-Fan X 2009 Proliferation, behavior, and cytokine gene expression of human umbilical vascular endothelial cells in response to different titanium surfaces *J. Biomed. Mater. Res.* A **93** 364–72
[35] Shi B, Andrukhov O, Berner S, Schedle A and Rausch-Fan X 2014 The angiogenic behaviors of human umbilical vein endothelial cells (HUVEC) in co-culture with osteoblast-like cells (MG-63) on different titanium surfaces *Dental Mater.* **30** 839–47
[36] Raines A L, Olivares-Navarrete R, Wieland M, Cochran D L, Schwartz Z and Boyan B D 2010 Regulation of angiogenesis during osseointegration by titanium surface microstructure and energy *Biomaterials* **31** 4909–17
[37] Blanchard F, Duplomb L, Baud'huin M and Brounais B 2009 The dual role of IL-6-type cytokines on bone remodeling and bone tumors *Cytokine Growth Factor Rev.* **20** 19–28
[38] Girasole G, Passeri G, Jilka R L and Manolagas S C 1994 Interleukin-11: a new cytokine critical for osteoclast development *J. Clin. Invest.* **93** 1516–24
[39] Hill P A, Tumber A, Papaioannou S and Meikle M C 1998 The cellular actions of interleukin-11 on bone resorption *in vitro Endocrinology* **139** 1564–72
[40] Petkovic A B *et al* 2010 Proinflammatory cytokines (IL-1beta and TNF-alpha) and chemokines (IL-8 and MIP-1alpha) as markers of peri-implant tissue condition *Int. J. Oral Maxillofac. Surg.* **39** 478–85
[41] O'Garra A, Barrat F J, Castro A G, Vicari A and Hawrylowicz C 2008 Strategies for use of IL-10 or its antagonists in human disease *Immunol. Rev.* **223** 114–31
[42] Buser D *et al* 2004 Enhanced bone apposition to a chemically modified SLA titanium surface *J. Dental Res.* **83** 529–33